Analysis of a Turbulent Lifted Hydrogen/Air Jet Flame from Direct Numerical Simulation with Computational Singular Perturbation

Tianfeng Lu[1]
Princeton University, Princeton, NJ 08544, USA

Chun S. Yoo[2], and Jacqueline H. Chen[3]
Sandia National Laboratories, Livermore, CA 94551, USA

Chung K. Law[4]
Princeton University, Princeton, NJ 08544, USA

The theory of computational singular perturbation (CSP) was employed to analyze the near-field structure of the stabilization region of a lifted hydrogen/air slot jet flame in a heated air coflow simulated with three-dimensional direct numerical simulation (DNS). The simulation was performed with a detailed hydrogen–air mechanism and mixture-averaged transport properties at a jet Reynolds number of 11,200 with approximately 1 billion grid points. Explosive chemical processes and their characteristic time scales, as well as the species involved, were identified by the CSP analysis of the Jacobian matrix of chemical source terms for species and temperature. An explosion index was defined for explosive modes, indicating the participation of species and temperature in the explosion process. Radical explosion and thermal runaway can consequently be distinguished. The CSP analysis of the simulated lifted flame shows the existence of two premixed flame fronts, which are difficult to detect with conventional methods. The upstream fork separating the two flame fronts thereby identifies the lift-off point. A Damköhler number was defined with the time scale of the chemical explosive mode and the scalar dissipation rate to show the role of auto-ignition in affecting the lift-off point and in stabilizing the flame.

I. Introduction

TURBULENT lifted flames are of relevance to the satisfactory operation of many practical devices. Consequently there have been extensive theoretical and experimental studies on lifted flames to understand their stabilization mechanism[1-7]. Several explanations have been offered based on the properties of premixed and non-premixed flames[2,5-7], auto-ignition[9,10], and turbulence–flame interactions[6,11,12]. However, the viability of most of the postulations is difficult to scrutinize due to difficulty in performing joint scalar-velocity measurements in turbulent reactive flows as well as the dearth of accurate simulation data reflecting the chemical response of key intermediate species to turbulent strain. Moreover, the associated utilities for analysis of mixed-modes of combustion are not concise.

Direct numerical simulation (DNS) is an information-rich platform for the study of turbulent lifted flames[13-15] by providing complete information of both the flow and the chemistry. Restricted by the high computation cost, fully 3-D DNS of hydrogen lifted flames with detailed kinetic mechanism became

[1] Research Staff, Department of Mechanical and Aerospace Engineering, AIAA Senior Member.
[2] Postdoctoral Researcher, Combustion Research Facility.
[3] Distinguished Member of Technical Staff, Combustion Research Facility.
[4] Robert H. Goddard Professor, Department of Mechanical and Aerospace Engineering, AIAA Fellow.

feasible only recently[16]. However, it remains a challenge to develop rigorous computational utilities to extract the salient information from the massive output of DNS.

In response to the above needs, in the present study the DNS results obtained in[16] are analyzed with a newly developed approach based on computational singular perturbation (CSP), which was developed in the mid 1980s[17-20]. Chemical explosive modes were identified and employed to extract premixed or partially premixed flame fronts from the simulated flow field, and to clearly identify the lifted flame stabilization mechanism in a vitiated coflow environment.

CSP was primarily applied in the analysis and reduction of stiff nonlinear ODEs, particularly those involving detailed chemical kinetics. It systematically identifies exhausted fast processes that algebraically relate the fast variables with others. In the past two decades, CSP has been widely adopted in various topics of mechanism reduction, such as the identification of quasi steady state (QSS) species[21-24], elimination of unimportant species and reactions[25], and stiffness removal[26-28]. It has also been applied to analyze complex flow–chemistry interaction[29], as well as biological systems[30]. CSP provides a refinement procedure to decouple the fast and slow processes iteratively until arbitrarily-high order of accuracy is achieved[19,32-34], and it degenerates to the method of intrinsic low dimensional manifold (ILDM)[35-38] if the time dependence of the Jacobian is neglected in decoupling the modes. In such cases, fast eigendecomposition of the Jacobian can be applied instead of the slow refinement procedure[23,35,39]. The eigendecomposition approach is simple to apply and has been found to be sufficiently accurate in many practical applications in mechanism reduction as well as flow simulations.

In addition to the refinement procedure, CSP provides two important concepts, namely the radical pointer and the participation index[19], which indicate the involvement of species and reactions, respectively, in the fast processes. In particular, the radical pointer can be employed to identify the candidate species to be solved by the algebraic equations. It has also been utilized in the identification of QSS species and the fast species induced by partial equilibrium reactions[21-24]. However, these concepts are not readily applicable to the study of chemical explosive modes, which is important for reactive flows involving ignition processes[39,40].

In the present study, concepts from CSP theory will be extended to study the stabilization and structure of a turbulent lifted hydrogen jet flame simulated by DNS. The role of the explosive chemical mode in flame front detection, from which the stabilization mechanism of the lifted flame can be understood, will be explored.

II. Methodology

A. A brief review of CSP

In the theory of CSP, a chemically reacting system is formulated as the following ODE:

$$\frac{d\mathbf{y}}{dt} = \mathbf{g}(\mathbf{y}) \quad , \tag{1}$$

where **g** is the source term, and **y** is the vector of dependent variables, such as species concentrations and temperature, that are nominally nonlinearly coupled in chemically reacting systems. Using the chain rule, Eq. (1) can be transformed to:

$$\frac{d\mathbf{g}}{dt} = \mathbf{J}\cdot\mathbf{g}(\mathbf{y}), \quad \mathbf{J} = \frac{d\mathbf{g}}{d\mathbf{y}} \quad , \tag{2}$$

where **J** is the Jacobian matrix. The variables in Eq.(2) can then be grouped using a basis change:

$$\frac{d\mathbf{f}}{dt} = \mathbf{\Lambda}\cdot\mathbf{f} \quad ,$$

$$\mathbf{f} = \mathbf{B}\cdot\mathbf{g} \quad ,$$

and

$$\mathbf{\Lambda} = (\frac{d\mathbf{B}}{dt} + \mathbf{B}\cdot\mathbf{J})\cdot\mathbf{A}, \quad \mathbf{A} = \mathbf{B}^{-1} \tag{3}$$

where **f** is the vector of modes, and matrices **A** and **B** consist of column and row basis vectors, respectively. In nonlinear systems, **J** is time dependent and so are **A** and **B**. In ideal cases, a diagonal **Λ** can be obtained from Eq. (3), such that each mode is completely decoupled from the others. For general cases, the ideal basis vectors are, however, not available, and CSP provides a refinement procedure[35, 36] to find a pair of **A** and **B** iteratively such that **Λ** is block-diagonal and consequently the fast and slow subspaces are decoupled:

$$\frac{d\mathbf{f}_{fast}}{dt} = \mathbf{\Lambda}_{fast}\mathbf{f}_{fast}, \quad \frac{d\mathbf{f}_{slow}}{dt} = \mathbf{\Lambda}_{slow}\mathbf{f}_{slow},$$

$$\mathbf{\Lambda} = \begin{pmatrix} \mathbf{\Lambda}_{fast} & \\ & \mathbf{\Lambda}_{slow} \end{pmatrix}, \quad \mathbf{A} = \begin{pmatrix} \mathbf{A}_{fast} & \mathbf{A}_{slow} \end{pmatrix}, \quad \mathbf{B} = \begin{pmatrix} \mathbf{B}_{fast} \\ \mathbf{B}_{slow} \end{pmatrix},$$

$$\mathbf{\Lambda}_{fast} = (\frac{d\mathbf{B}_{fast}}{dt} + \mathbf{B}_{fast}\cdot\mathbf{J})\cdot\mathbf{A}_{fast}, \quad \mathbf{\Lambda}_{slow} = (\frac{d\mathbf{B}_{slow}}{dt} + \mathbf{B}_{slow}\cdot\mathbf{J})\cdot\mathbf{A}_{slow}. \tag{4}$$

The CSP refinement ensures that the eigenvalues of $\mathbf{\Lambda}_{fast}$ are all negative and have much larger magnitude than that of $\mathbf{\Lambda}_{slow}$, such that the fast modes are exhausted after a transient period. *i.e.*

$$\mathbf{f}_{fast} = \mathbf{0}. \tag{5}$$

Once the fast modes are identified, the species involving the fast subspace can be identified using radical pointers, defined as:

$$\mathbf{Q} = diag(\mathbf{A}_{fast}\mathbf{B}_{fast}), \tag{6}$$

where Q_i indicates how parallel the i^{th} variable, which can be either a species or temperature, is to the fast subspace. A variable is a CSP radical if its radical pointer is not small, and CSP radicals are the candidates that can be solved by the algebraic equations in (5)[1]. It is noted that although radical pointers are normalized, they can be negative or larger than unity. Therefore special care is needed when comparing radical pointers with threshold values.

Practically, the time dependence of matrix **B** is difficult to compute in Eq. (3), and was frequently neglected when leading order accuracy is adequate. In such cases, Eq. (3) can be replaced by simple eigendecomposition[23,35,39]. *i.e.*

$$\mathbf{\Lambda} = \mathbf{B}\cdot\mathbf{J}\cdot\mathbf{A}, \quad \mathbf{A} = \mathbf{B}^{-1}, \tag{7}$$

and **Λ** is diagonal if **J** is not defective, such that the modes are fully decoupled with leading order accuracy. Complex eigenvalues of **J** indicate the existence of oscillatory modes[23], the significance of which has been investigated for the ignition of large hydrocarbons[39]. Nonetheless, the study of chemical explosive modes with CSP has only been preliminary, and it has not yet been applied to turbulent reactive flows. In the following sections, concepts from CSP will be employed to investigate the role of explosive modes in homogeneous as well as diffusive flows, and a new approach for flame front detection in an autoignitive flow will be proposed.

B. Quantification of Explosive Modes

Explosive modes are those associated with positive eigenvalues of the Jacobian. *i.e.*

$$real(\lambda_{\exp}) > 0, \tag{8}$$

where λ_{exp} is a diagonal element of $\mathbf{\Lambda}$. A complex λ_{exp} indicates an oscillatory mode. The real part of λ_{exp} is the reciprocal time scale of the explosion, and the imaginary part is the oscillation frequency. In the present study, we shall focus on only the real part of λ_{exp}. Once the explosive mode is identified, a concept similar to the radical pointer can be defined:

$$\mathbf{E} = diag(\mathbf{A}_{\exp}\mathbf{B}_{\exp}), \tag{9}$$

where $\mathbf{A}_{\exp}$ and $\mathbf{B}_{\exp}$ are the eigenvectors associated with λ_{exp}. Similarly, $\mathbf{E}$ is non-dimensional and its ith entry, E_i, indicates how parallel the ith variable is to the explosive mode. To avoid confusion with the radical pointer, $\mathbf{E}$ will be called "explosion pointer" in the present work.

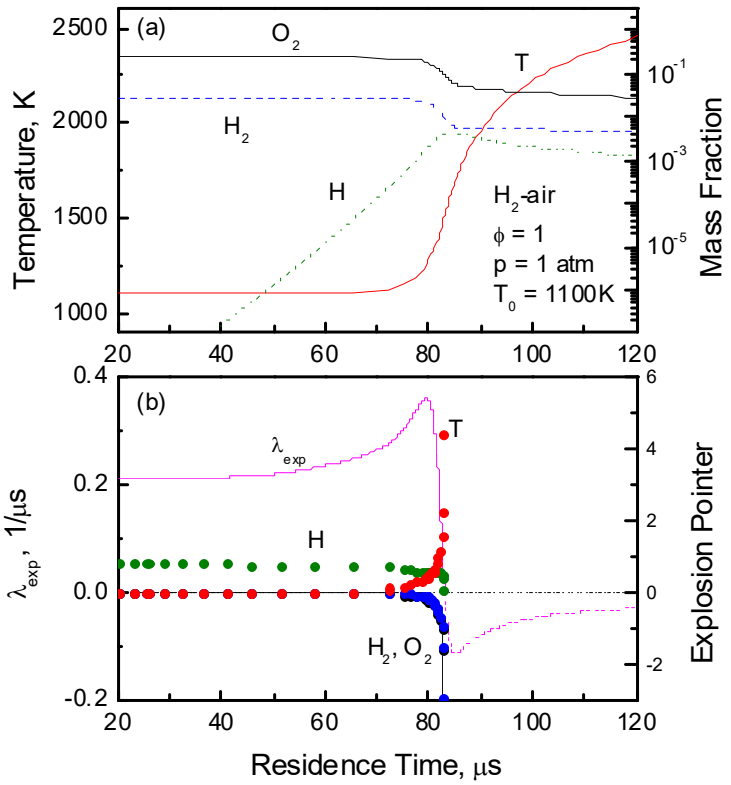

Figure 1. Temperature and selected species profiles in auto-ignition of a stoichiometric hydrogen-air mixture under atmospheric pressure and initial temperature of 1100K. (a) temperature and species concentrations, and (b) time scale of the explosive mode (solid line) and the explosion pointer (dotted line lines).

The existence of explosive modes and the concept of the explosion pointer is demonstrated in Fig. 1 for the homogeneous auto-ignition of a stoichiometric hydrogen–air mixture. The detailed hydrogen–air kinetic mechanism is from Li *et al.*[41]. Figure 1a shows the temperature and mass fraction of selected species, namely H, H_2, and O_2, and Fig. 1b shows the time scale of the explosive mode and the explosion pointers. An interesting observation in Fig 1b is that the explosion pointers of temperature and fuel diverge as they approach the inflection point in the temperature profile, indicating the existence of a singularity where the eigenvalue of the explosive mode crosses zero. It is noted that, while not shown in Fig. 1, a similar trend was also observed for hydrogen and hydrocarbon fuels under a variety of conditions. To explain this observation, it is further observed in Fig. 1b that, while the explosion pointer of temperature grows positively near the singularity, that of the reactants, i.e. H_2 and O_2, grows on the negative side, indicating that the effect of thermal runaway is balanced by the consumption of reactants at the crossover point. A closer inspection of the eigenvector of the explosive mode shows that the explosive mode rotates into the

direction of the energy conservation mode through thermal runaway, such that the Jacobian becomes defective at the crossover point. Therefore, although the entries in **E** sum to unity, each explosion pointer may be arbitrarily large near ignition, rendering it difficult to use. To resolve this problem, the explosion pointers defined in Eq. (9) are further normalized in the present study:

$$\mathbf{EI} = \frac{|\mathbf{E}|}{\sum_{j=1}^{N} |E_j|}, \tag{10}$$

where for distinction the explosion index is denoted by **EI**. It is noted that, although the explosion indices are normalized to [0, 1] in Eq. (10), it should not be evaluated too close to the singularity because of the large numerical errors induced by the inversion of an ill-conditioned matrix **A**.

Figure 2 shows the explosion index for temperature and species with nontrivial participation in the explosive mode for the auto-ignition case of Fig. 1. It is seen that there are two stages in the ignition process, namely radical explosion and thermal runaway. The radical explosion stage occurs before approximately 70μs. It is dominated by the H radical whereas the temperature effect is negligible. Thermal runaway occurs near the very end of the ignition process, where temperature is significantly involved and the contribution from H vanishes. The two ignition stages are therefore naturally divided at the point where the explosion index of temperature becomes larger than that of the radicals, as shown in Fig. 2. The radical explosion stage is manifested by the exponential growth in H radical in a nearly isothermal environment as shown by the linear segment in Fig. 1a. In Fig. 1b, it is observed that the time scale of the explosive mode remains almost unchanged during radical explosion, and varies dramatically during thermal runaway. The mixture becomes non-explosive once it passes the inflection point.

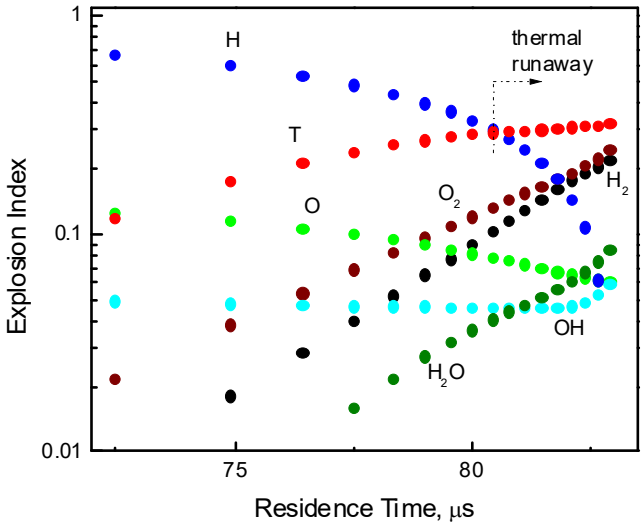

Figure 2. Explosion index for temperature and species in auto-ignition of stoichiometric hydrogen-air mixture under atmospheric pressure and initial temperature of 1100K. The explosion indices for HO_2 and H_2O_2 are negligible and not shown.

Since explosivity is a chemical property of the mixture, the time scale of explosive modes and the explosion indices can be utilized to distinguish between unburned and burned mixtures, not only in homogeneous applications, but also in diffusive systems. This is because explosive modes in diffusive systems are induced by the chemical source term rather than by diffusion, since diffusion is dissipative in nature. Therefore, the eigenanalysis in Eqs. (1) - (10) can be performed only on the Jacobian matrix of the chemical source term to detect the explosivity of the mixture. For demonstration, Fig. 3 shows the structure and the profile of the chemical explosive mode in a 1-D freely propagating laminar premixed flame. Note that the explosive mode only exists in the preheat zone where the mixture is unburned. The time scale for the explosive mode first increases as temperature rises, and then quickly vanishes when the mixture is burned. Similar to Fig. 1b, the transition from an explosive to a non-explosive mixture occurs abruptly, forming a boundary that is much thinner than the flame thickness, and sharply separating the two types of mixtures. To further verify the validity of this measure over a wide range of mixtures, the temperature profiles of lean to rich premixed H_2-air flames are plotted in Fig. 4, with timescales of the explosive modes superimposed in color. Note that, for each of the five cases, the transition from explosive to non-explosive

mixture is abrupt, while the change within the unburned zone is smooth. Therefore, the sharp boundary is a general property of a premixed flame and can be utilized to detect premixed flame fronts in more complex flow fields.

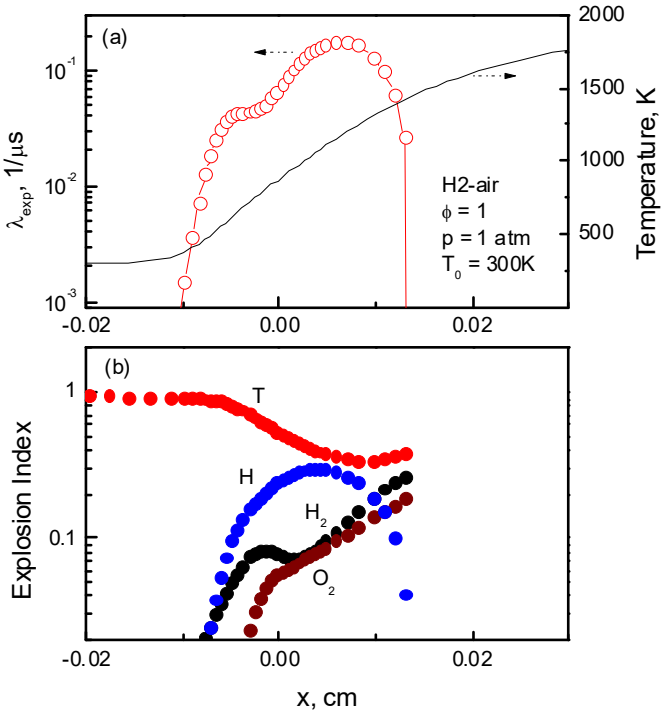

Figure 3. Explosive mode in a 1-D freely propagating laminar premixed flame with a stoichiometric H_2-air mixture under STD. (a) time scale of the explosive mode and temperature profile. (b) explosion index of temperature, H, H_2 and O_2.

Another interesting observation for pre-mixtures can be seen in Fig. 3b, which shows the explosion indices for temperature and species. In contrast to the homogeneous ignition in Figs. 1-2, no radical explosion stage is observed for the flame. The explosion index of temperature dominates the entire preheat zone, although the radical H still moderately participates in the explosion. This is because the strong diffusion of the H radical from the burned mixture dominates the local generation of H in the preheat zone, such that radical explosion is not important in building up the radical pool in the preheat zone. This observation can be useful in detecting whether a reaction front is dominated by flame propagation or by auto-ignition.

We now extend these observations in homogeneous and diffusive systems to analyze the region near the flame base of a turbulent lifted flame in a heated coflow computed by DNS.

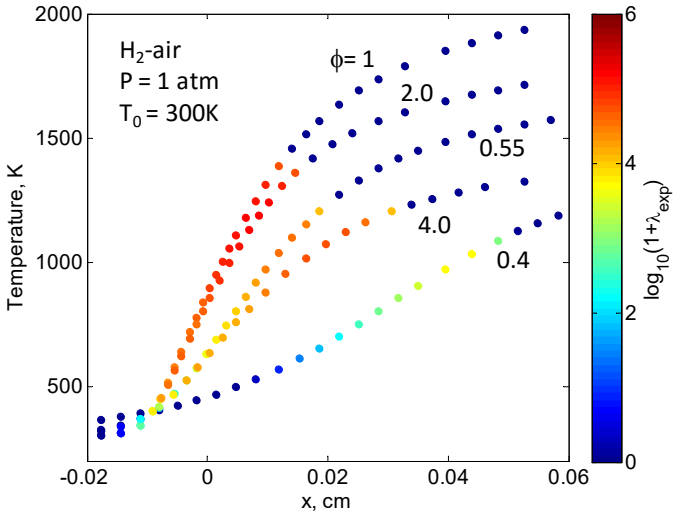

Figure 4. Temperature profiles of H_2-air mixtures for different equivalence ratios, colored with the time scales of the explosive modes.

III. Results and Discussions

A. Configuration and Selected Results of the DNS

A description of the detailed configuration of the DNS can be found in Ref. [16]. To summarize, three-dimensional DNS of a turbulent lifted hydrogen jet flame in a heated coflow was performed using a Sandia DNS code, S3D. S3D solves the compressible Navier-Stokes equations with a fourth-order explicit Runge-Kutta method for time integration, and an eighth-order centered finite difference scheme for spatial differentiation. The detailed kinetic mechanism used in the DNS is from Ref. [41]. The inlet fuel jet consists of 65% hydrogen and 35% nitrogen by volume under atmospheric pressure, at a temperature of 400K, and with a jet velocity of 347m/s. The coflowing air is at 1100 K and has a velocity of 4m/s. The jet Reynolds number is 11,200 based on the width of the slot, which is 1.92mm. The size of the domain is 24mm by 32mm by 6.4mm in streamwise (x), transverse (y) and spanwise (z) directions, respectively, and was discretized to 944 million grid points. The grid resolution is sufficient to resolve both the Kolmogorov and flame/ignition structure. The DNS assumes nonreflecting inflow/outflow boundary conditions in the streamwise and transverse directions, and periodic boundary conditions in the spanwise direction. The flow field was artificially ignited at $t = 0$ and was integrated with constant time steps of 4ns until the flame became statistically stationary, in less than about 1ms. Subsequently, the simulation was integrated for several more flow through times to provide statistics for model validation and development. The DNS was performed on a 50-110 Tflop Cray XT3/XT4 at Oak Ridge National Laboratories, and used approximately 3.5 million CPU-hours on 9,000 processors. A representative two-dimensional spanwise slice at $t = 0.84$ms and z = 6.4mm was selected from the 30 terabytes of raw data to be analyzed in the following.

Figure 5 shows the spatial profiles of selected results from the DNS. The left panels include temperature, mixture fraction computed with Bilger's formula[42], and heat release rate. The right panels show the concentrations of the important radicals. First, it is seen that the simulation provides abundant information to facilitate the understanding of the structure of the lifted flame. For example, the temperature panel shows three bulk regions: unburned cold fuel near the jet center (blue), preheated air (cyan), and the burned mixtures in the mixing layer (red). Therefore the position where the flame starts can be roughly determined as the leading edge of the high temperature zone. The panel of the mixture fraction further shows the structure of the mixing layer. It is not surprising that high temperature is observed in well-mixed regions, and the highest temperature is correlated with slightly rich mixtures with mixture fractions between ~0.2-0.3, where the stoichiometric mixture fraction, $\xi_{st} = 0.1990$. The distribution of the heat release rate peaks mostly near the leading edge of the mixing layer with high temperatures. Due to the Arrhenius effect, the reaction rate is very sensitive to temperature fluctuations. Furthermore, fast reactions typically cannot sustain themselves due to the rapid depletion of the reactants, as such large reaction rates are typically transient, resulting in the presence of distributed small hotspots on the heat release plot.

The right panels consist of the profiles for H, OH and HO_2, respectively. H is a crucial radical for hydrogen and hydrocarbon fuels, and high concentration of H typically indicates strong chemical reactions, which are again strongly affected by temperature. Therefore a clear correlation of H and temperature can be observed. Next, we note that OH is an important experimental flame marker, and it is a fairly good quasi-steady state species[43]. Its concentration strongly depends on both temperature and the concentration of H. Moreover, H and OH typically peak in the reaction zone of flames and slowly diminish in the recombination zone where temperature approaches the adiabatic value. Therefore, the zones with high concentrations of H and OH roughly resemble that of high temperature, but with some offset in their maximum positions. In contrast to H and OH, HO_2 typically peaks prior to ignition and is quickly depleted in ignited mixtures. As such, HO_2 is a good indicator of on-going ignition processes. From the bottom-right panel of Fig. 5, note that, with the exception near the flame stabilization point, HO_2 peaks primarily in the unburned fuel-rich mixtures in the central jet. Near the stabilization point, HO_2 peaks in the ignitive fuel-lean, high-temperature mixture.

Nonetheless, although the quantities plotted in Fig. 5 are very helpful in understanding the basic structure of the lifted flame, there is insufficient information to locate the exact positions of the flame fronts and the lift-off point in the flow field. First, this is because flame fronts are typically very thin and there is no clearly visible thin boundary in any of the panels of Fig. 5. Second, most of the quantities shown in Fig. 5 are severely affected by the local equivalence ratio, which spans a wide range from extremely lean to extremely rich in the flow field, and as such, the plots in Fig. 5 are biased. Therefore, the lean flames, if they exist at all, are very difficult to discern from the flame measureables shown in Fig. 5, due to the extremely lean flammability limit of hydrogen.

Next, we shall employ the method of explosive mode analysis for the effective detection of flames, particularly the lean fronts, which consequently reveals the stabilizing mechanism of the lifted flame.

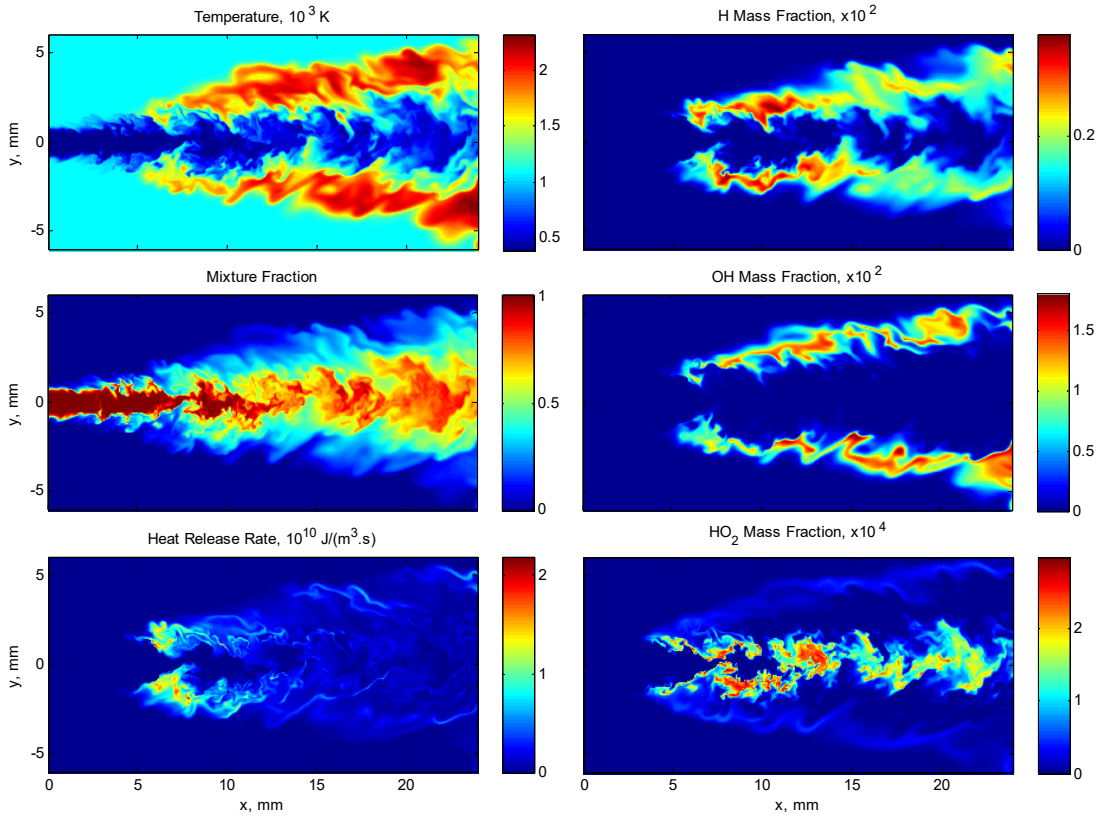

Figure 5. The spatial distribution of temperature, mixture fraction, heat release rate, and species mass fractions from the DNS result of the H_2 jet into pre-heated air at t = 0.84ms and z = 6.4mm.

B. Explosive Mode Analysis

The explosive mode analysis in Section 2 was performed at each grid point in the flow field. The eigenvalue, or the reciprocal time scale, of the explosive mode is plotted in Fig. 6. It is noted that modes with time scales longer than 1s are considered non-explosive because it is basically dormant within a flow-through time, which is about 0.07ms. It is seen from Fig. 6 that the entire domain can be classified into two types of regions: the non-explosive region denoted by the blue background, and the explosive region denoted by warmer colors. The non-explosive region is comprised of three zones: the fuel-lean heated air coflow outside of the central jet, the cold fuel-rich turbulent central jet, and the pair of mixing layers downstream of the lift-off region containing near-equilibrium combustion products. The first two

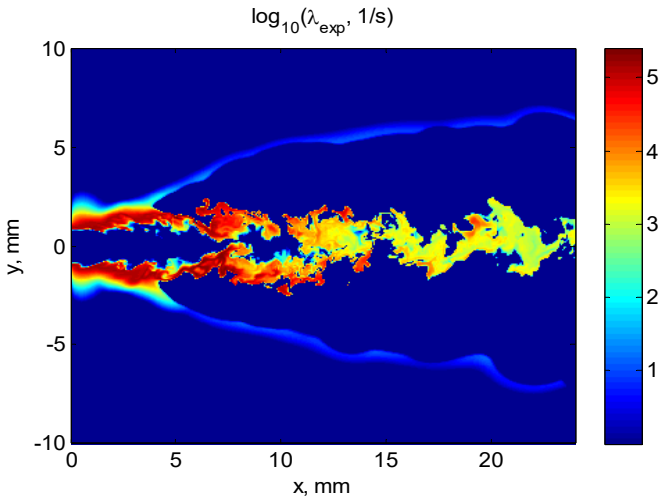

Figure 6. Spatial distribution of the time scale of local chemical explosive mode from the DNS result of the H_2 jet into pre-heated air at t = 0.84ms and z = 6.4mm. Time scales longer than 1s were truncated to 1s.

zones are basically non-explosive as the mixtures exceed the lean and rich flammability limits, respectively. Note, that the downstream burnt gas mixing layers are enclosed by sharp boundaries, whereas the upstream fuel and oxidizer zones do not exhibit a sharp boundary separating non-explosive from explosive zones. In the absence of a flame front, the upstream zones rely on diffusive mixing, and hence, there exists a gradual transition from non-explosive to explosive mixtures. The pair of non-explosive zones in the mixing layer enclose high temperature mixtures shown in Fig. 5, and are separated by sharp boundaries from the explosive mixtures. These sharp boundaries are attributed to premixed flame fronts separating the burned and unburned mixtures, similar to the abrupt change from explosive to non-explosive mixture in a laminar premixed flame shown previously in Fig. 3. It is further observed that there are two major segments of flame fronts, one close to the central fuel-rich jet, and the other on the air side with lean mixtures. The rich flame front is severely corrugated due to the intense turbulence in the central jet, and the lean flame front is nearly laminar as it exists in the heated coflow where the turbulence is dissipated.

Note that the rich flame fronts delineated by the explosive mode analysis are similar to those delineated by high HO_2 concentrations shown in Fig. 5. However, the lean flame fronts are only visible from the explosive mode plot because the mixture is very lean, particularly far downstream, where the temperature is close to the ambient value, and the fuel and radicals exist in very low concentrations. Furthermore, the leading edges of the lean and rich boundaries merge near the position where hot, burned mixtures appear. The upstream branching point denotes the stabilization, or lift-off, point, where the first parcel of mixture ignites. The mixture upstream of this point is very lean, with almost ambient temperature, such that the temperature rise downstream of this location is not readily visible from the temperature field shown in Fig. 5.

Upstream from each stabilization point, a stream of highly explosive mixtures is observed starting from the nozzle exit. Rough measurement shows that the time scale of the explosive mixture is comparable to the flow time from the nozzle exit to the stabilization point, implying that auto-ignition, rather than flame propagation, is the controlling factor determining the lift-off height. To further prove this point, we define a Damköhler number as:

$$Da = \lambda_{\exp} \cdot \chi \,, \tag{11}$$

,where χ is the scalar dissipation rate. The Damköhler number, therefore, indicates how fast the explosive mode is compared with transport. If Da>>1, chemical explosion is much faster than mixing, and hence, the mixture is dominated by auto-ignition. Otherwise, chemical explosion can be severely altered by mixing. The Da field plotted in Fig. 7, resembles that of the eigenvalue plot in Fig. 6, and clearly shows two thin wrinkled layers of auto-igniting mixtures (in dark red), each of which ends at a stabilization point. The mechanism of lifting points induced by auto-ignition is hereby clear. Moreover, premixed flame fronts can be defined at the boundary of Da = 1, i.e., where chemical explosion is balanced by mixing. This criterion is advantageous over the eigenvalue plot, because the threshold value is normalized. Nonetheless, the flame fronts depicted by Da and those by the eigenvalues are almost identical.

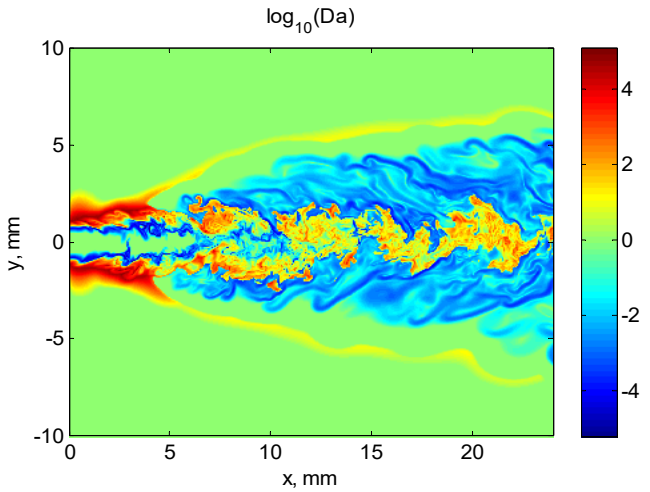

Figure 7. Spatial distribution of the Damköhler number from the DNS result of the H_2 jet into pre-heated air at t = 0.84ms and z = 6.4mm. Time scales longer than 1s were truncated to 1s for both the explosive mode and the scalar dissipation rate.

Finally, to show that the stabilization point is not primarily affected by flame propagation, the explosion index, defined in Eq. (10), is plotted in Fig. 8 for H radical and temperature, respectively. As discussed in Fig. 3, radical explosion is not important in the flame preheat zone, while it is a necessary precursor to the accumulation of a radical pool for auto-ignition.

Therefore, a typical premixed flame front is preceded by a rather wide thermal runaway zone, while the thermal runaway zone for auto-ignition is relatively thinner, as shown in Fig. 1b. In Fig. 8, it is clearly observed that radical explosion dominates almost the entire stream of the highly explosive mixture leading to the stabilization point, whereas thermal runaway is observed only in the vicinity of the stabilization point.

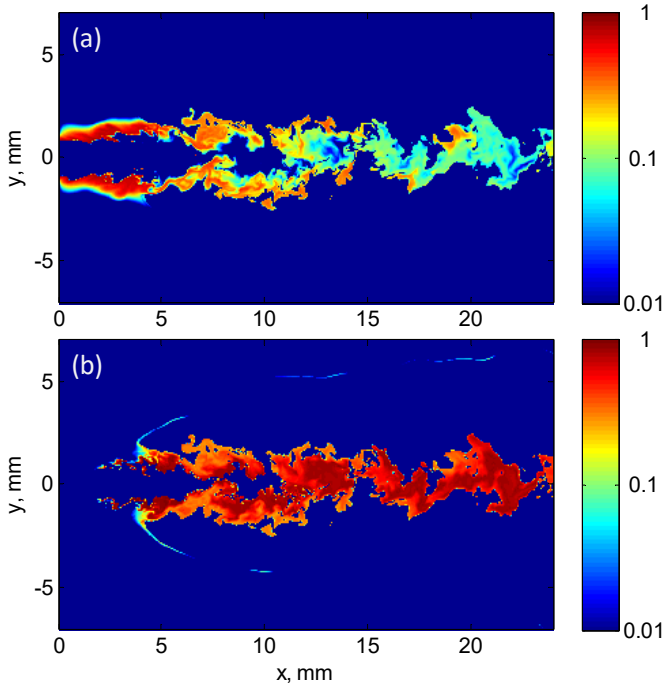

Figure 8. Spatial distribution of the Explosion Index for (a) H radical, and (b) temperature, respectively.

In summary, the stabilization mechanism of the lifted hydrogen flame in heated coflow occurs by: the reactants are mixed at nozzle exit and form a thin layer of lean mixture at close-to-ambient temperature. This most explosive layer of mixture is then convected downstream as the radical pool is built up in a near-homogeneous environment. The mixture finally ignites at the lift-off point after transient thermal runaway. The leading edge of the two premixed flames are formed, one propagating to the lean side and the other to the rich, and the mixture loses its explosivity thereafter. The lean flame propagates outward from the mixing layer and decelerates as it approaches the lean flammability limit, where the flow is laminar. The rich flame propagates toward the jet center until it reaches the rich flammability limit. The rich flame front is severely wrinkled and disrupted by the intense turbulence, and islands of burned and unburned mixtures are formed.

C. Comparison with Flame Index

Takeno's flame index[44] has been a useful measure to delineate between premixed and non-premixed flame fronts in complex flow fields. The flame index is defined as:

$$FI = \nabla Y_F \cdot \nabla Y_O , \tag{12}$$

where F denotes the fuel and O the oxidizer. In premixed flames the gradients of fuel and oxidizer are aligned, such that the rapid consumption of the reactants across the flame results in a large positive value of flame index. In non-premixed flames the gradients of fuel and oxidizer oppose one another, and the flame index is negative. The magnitude of the flame index increases as the flame becomes thinner.

The concept of flame index is different from the current method of explosive mode analysis in several aspects. First, the explosive mode is a chemical property of the mixture while the flame index is not. Therefore the flame index may also peak in nonreactive flows, such as premixed or non-premixed opposed jets, particularly where the scalar field is subjected to intense stretch. Therefore, a flame may not exist at all

where the flame index peaks. Second, the flame index is dimensional, and it can be difficult to select a threshold value for complex flows, whereas the simple criterion of $Da = 1$ can be applied in the present method. Third, the flame index suffers from similar problems as the other quantities plotted in Fig. 5, *i.e.* the plot may be biased and difficult to use for extremely lean mixtures. This problem, however, is readily handled by the explosive mode analysis. To demonstrate the above points, the flame index for the lifted flame is shown in Fig. 9, superimposed with an isocontour corresponding to a timescale of an explosive mode from Fig. 6. It is seen that negative peaks of the flame index are observed in the mixing layer before the lift-off point, where no flame exists, and these peaks are induced by the strained mixing process. Furthermore, the lean flame fronts are not visible in the flame index plot because of the bias induced by the local equivalence ratio.

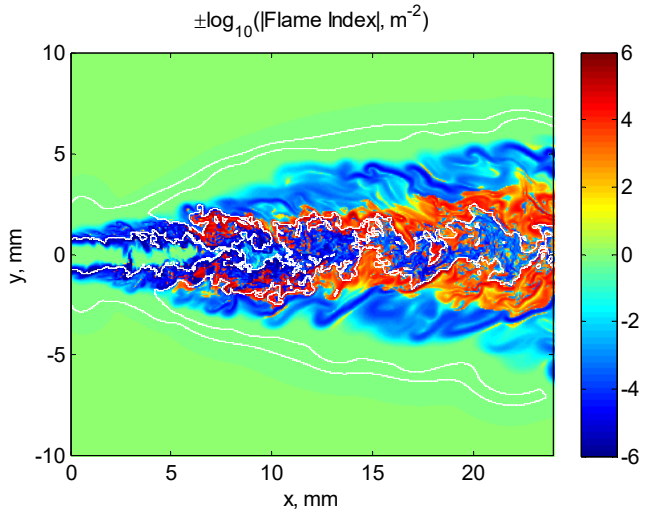

Figure 9. Spatial distribution of flame index from the DNS result of the H_2 jet into pre-heated air at t = 0.84ms and z = 6.4mm, superimposed with the isocontour of λ_{exp} = 1/s from Fig. 6. Flame index smaller than 1/m^2 were truncated.

IV. Conclusions

In summary, explosive modes in chemically reacting flows were studied based on CSP. The abrupt change in the mixture explosivity was employed for the detection of premixed flame fronts, which was found to be difficult using conventional methods involving only individual parameters such as temperature, mixture fraction, heat release rate, and species concentrations. A singular eigenvector matrix induced by vanishing explosive modes was observed, and it was found that the singularity is caused by the convergence of the explosive mode to the mode of energy conservation. A species explosion index was consequently defined to normalize the diverging explosion pointers near the singularity. Radical explosion and thermal runaway were then distinguished with the explosion pointers. The present method was first tested on homogeneous auto-ignition and 1-D laminar premixed flames, and subsequently applied to a turbulent lifted hydrogen jet flame simulated with DNS. Lean laminar and rich turbulent flame fronts were detected, and the point of intersection leading the two flame fronts was identified as the lift-off point. A Damköhler number based on the time scale of the explosive mode and the scalar dissipation rate was defined to identify auto-igniting mixtures, and the role of auto-ignition as the mechanism for stabilization of the lifted flame was discussed.

It is noted that, although the present method was successfully applied in the analysis of the present lifted flame, it only detects premixed or partially premixed flames in that the fuel and oxidizer need to be premixed to be explosive. When non-premixed flames, such as the trailing diffusion flame zone enclosed by the lean and rich premixed flame fronts in the present study, are of interest, additional methodology is required.

In addition to lifted flames, explosive chemical modes can also provide useful information in other flow analysis, such as those involving the competing effects of flame and ignition front propagation during reignition following local extinction in highly strained turbulent nonpremixed flames. It is also important in the study of the turning points on extinction and ignition curves for steady state flows. Such topics can be interesting extensions of the present study.

Acknowledgement

The work at Princeton University was supported by the Air Force Office of Scientific Research under the technical monitoring of Dr. Julian M. Tishkoff. The work at Sandia National Laboratories (SNL) was supported by the Division of Chemical Sciences, Geosciences, and Biosciences, Office of Basic Energy Sciences of the U. S. Department of Energy, and the U. S. Department of Energy SciDAC Program. SNL is a multiprogram laboratory operated by Sandia Corporation, a Lockheed Martin Company, for the U. S. Department of Energy under contract DE-AC04-94AL85000. The simulation used resources of the National Center for Computational Sciences (NCCS) at ORNL, which is supported by the Office of Science of the U.S. DOE under contract DE-AC05-00OR22725.

References

[1] L. Vanquickenborne and van A. Tiggelen, "The Stability Mechanism of Lifted Diffusion Flames," *Combust. Flame*, 10 (1966) 59−69.

[2] N. Peters and F. A. Williams, "Liftoff Characteristics of Turbulent Jet Diffusion Flames," *AIAA J.*, 21 (1983) 423−429.

[3] G.T. Kalghatgi, "Lift-off Heights and Visible Lengths of Vertical Turbulent Jet Diffusion Flames in Still Air," *Combust. Sci. Technol.*, 41 (1984) 17−29.

[4] W.M. Pitts, "Assessment of Theories for the Behavior and Blowout of Lifted Turbulent Jet Diffusion Flames", *Proc. Combust. Inst.*, 22 (1988) 809−816.

[5] A. Upatnieks, J.F. Driscoll, C.C. Rasmussen, and S.L. Ceccio, "Liftoff of Turbulent Jet Flames − Assessment of Edge Flame and Other Concepts Using Cinema-PIV," *Combust. Flame*, 138 (2004) 259−272.

[6] A. Joedicke, N. Peters, and M. Mansour, "The Stabilization Mechanism and Structure of Turbulent Hydrocarbon Lifted Flames," *Proc. Combust. Inst.*, 30 (2005) 901−909.

[7] S. H. Chung, "Stabilization, propagation and instability of tribrachial triple flame", Proc. Combust. Inst., 31, 877−892 (2007).

[8] K.M. Lyons, "Toward an Understanding of the Stabilization Mechanisms of Lifted Turbulent Jet Flames: Experiments", *Prog. Energy Combust. Sci.*, 33 (2007) 211−231.

[9] R. Cabra, T. Myhrvold, J.Y. Chen, R.W. Dibble, A.N. Karpetis, and R.S. Barlow, "Simultaneous Laser Raman-Rayleigh-LIF Measurements and Numerical Modeling Results of a Lifted Turbulent H2/N2 Jet Flame in a Vitiated Coflow," *Proc. Combust. Inst.*, 29 (2002) 901−909.

[10] C.N. Markides and E. Mastorakos, "An Experimental Study of Hydrogen Autoignition in a Turbulent Co-Flow of Heated Air," *Proc. Combust. Inst.*, 30 (2005) 883−891.

[11] M.M. Tacke, D. Geyer, E.P. Hassel, and J. Janicka, "A Detailed Investigation of the Stabilization Point of Lifted Turbulent Diffusion Flames," *Proc. Combust. Inst.*, 27, (1998) 1157−1165.

[12] L.K. Su, O.S. Sun, and M.G. Mungal, "Experimental Investigation of Stabilization Mechanisms in Turbulent, Lifted Jet Diffusion Flames," *Combust. Flame*, 144 (2006) 494−512.

[13] H. Yamashita, M. Shimada, and T. Takeno, "A Numerical Study on Flame Stability at The Transition Point of Jet Diffusion Flames," *Proc. Combust. Inst.*, 26 (1996) 27–34.

[14] C. Jiménez and B. Cuenot, "DNS Study of Stabilization of Turbulent Triple Flames by Hot Gases," *Proc. Combust. Inst.*, 31 (2007) 1649–1656.

[15] Y. Mizobuchi, S. Tachibana, J. Shinio, and S. Ogawa, "A Numerical Study on The Formation of Diffusion Flame Islands in A Turbulent Hydrogen Jet Lifted Flame," *Proc. Combust. Inst.*, 30 (2005) 611–619.

[16] C.S. Yoo, J.H. Chen, and R. Sankaran, "A 3D DNS Study of the Stabilization of a Turbulent Lifted Hydrogen/Air Jet Flame in an Autoignitive Heated Coflow," *Fall Meeting of the Western States of the Combustion Institute*, Sandia National Laboratories, Livermore, USA, Paper # 07F57, 2007.

[17] S.H. Lam, "Singular Perturbation for Stiff Equations Using Numerical Methods," *Recent Advances in the Aerospace Sciences*, Eds. Corrado Casci in honor of Luigi Crocco, Plenum Press, New York and London, 1985.
[18] S.H. Lam, *Combust. Sci. and Tech.*, 89 (1993) 375-404.
[19] S.H. Lam and D.A. Gousis, *Int. J. Chem. Kinetic*., 26 (1994) 461-486.
[20] S.H. Lam, "Reduced Chemistry-Diffusion Coupling," *Combust. Sci. and Tech.*, 179 (4) (2007) 767–786.
[21] A. Massias, D. Diamantis, E. Mastorakos, and D.A. Goussis, *Combust. Flame*, 117 (4) (1999) 685-708.
[22] A. Massias, D. Diamantis, E. Mastorakos, and D.A. Goussis, *Combust. Theory Modelling*, 3(1999) 233–257.
[23] T.F. Lu, Y. Ju, and C.K. Law, "Complex CSP for Chemistry Reduction and Analysis," *Combust. Flame* 126 (1-2) (2001) 1445-1455.
[24] T.F. Lu, and C.K. Law, "Strategies for Mechanism Reduction for Large Hydrocarbons: n-Heptane," *Combust. Flame*, in press.
[25] M. Valorani, F. Creta, D.A. Goussis, J.C. Lee, H.N. Najm, "An Automatic Procedure for the Simplification of Chemical Kinetic Mechanisms Based on CSP," *Combust. Flame*, 146 (1-2) (2006) 29–51.
[26] M. Valorani, D.A. Goussis, F. Creta, H.N. Najm, "Higher Order Corrections in the Approximation of Low-Dimensional Manifolds and the Construction of Simplified Problems with the CSP Method," *J. Comput. Phys.*, 209 (2005) 754–786.
[27] D.A. Goussis, M. Valorani, "An Efficient Iterative Algorithm for the Approximation of the Fast and Slow Dynamics of Stiff Systems," *J. Comput. Phys.*, 214 (2006) 316–346.
[28] J.C. Lee, H.N. Najm, S. Lefantzi, J. Ray, M. Frenklach, M. Valorani, and D.A. Goussis, "A CSP and Tabulation-based Adaptive Chemistry Model," *Combust. Theory Modelling*, 11 (1) (2007) 73-102.
[29] M. Valorani, H.N. Najm, D.A. Goussis, "CSP Analysis of a Transient Flame-Vortex Interaction: Time Scales and Manifolds," *Combust. Flame*, 134 (2003) 35–53.
[30] D.A. Goussis, and H.N. Najm, "Model Reduction and Physical Understanding of Slowly Oscillating Processes: The Circadian Cycle," *Multiscale Model. Simul.*, 5 (4) (2006) 1297-1332.
[31] H.G. Kaper, and T.J. Kaper, "Asymptotic Analysis of Two Reduction Methods for Systems of Chemical Reactions," *Physica D*, 165 (2002) 66–93.
[32] A. Zagaris, H.G. Kaper, T.J. Kaper, *J. Nonlinear Sci.*,14 (1) (2004) 59–91.
[33] A. Zagaris, H.G. Kaper, and T.J. Kaper, "Two Perspectives on Reduction of Ordinary Differential Equations," *Math. Nachr.*, 278 (12–13) (2005) 1629 – 1642.
[34] A. Zagaris, H.G. Kaper, and T.J. Kaper, "Fast and Slow Dynamics for the Computational Singular Perturbation Method," *Multiscale Model. Simul.*, 2(4) (2004) 613–638.
[35] U. Maas and S.B. Pope, *Combust. Flame.* 88 (3-4) (1992) 239-264.
[36] Z. Ren and S.B. Pope, "The Use of Slow Manifolds in Reactive Flows," *Combust. Flame*, 147 (4) (2006) 243-261.
[37] Z. Ren and S.B. Pope, "Reduced Description of Complex Dynamics in Reactive Systems," *J. Phys. Chem. A*, 111 (2007) 8464-8474.
[38] Z. Ren and S.B. Pope, "Transport-Chemistry Coupling in the Reduced Description of Reactive Flows," *Combust. Theory Modelling*, 11 (5) (2007) 715-739.
[39] A. Kazakov, M. Chaos, Z. Zhao, and F.L. Dryer, "Computational Singular Perturbation Analysis of Two-Stage Ignition of Large Hydrocarbons," *J. Phys. Chem. A*, 110 (2006) 7003-7009.
[40] C.G. Fotache, T.G. Kreutz, and C.K. Law, "Ignition of Counterflowing Methane versus Heated Air under Reduced and Elevated Pressures," *Combust. Flame*, 108 (1997) 442-470.
[41] J. Li, Z. Zhao, A. Kazakov, and F.L. Dryer, "An Updated Comprehensive Kinetic Model of Hydrogen Combustion," *Int. J. Chem. Kinetic*., 36 (10) (2004) 566-575.
[42] R.W. Bilger, "The Structure of Turbulent Nonpremixed Flames," *Combust. Flame*, 22 (1998) 475–488.
[43] T.F. Lu, C.K. Law, and Y. Ju, "Some Aspects of Chemical Kinetics in C-J Detonation: Induction Length Analysis," *J. Propulsion Power*, 19(5) (2003) 901-907.
[44] H. Yamashita, M. Shimada, and T. Takeno, "A Numerical Study on Flame Stability at the Transition Point of Jet Diffusion Flames," *Proc. Combust. Inst.*, 26 (1996) 27–34.